The EMBO Journal vol.12 no.3 pp.837-847, 1993

Initiation of assembly and association of the structural elements of a bacterial pilus depend on two specialized tip proteins

Françoise Jacob-Dubuisson, John Heuser[1], Karen Dodson, Staffan Normark and Scott Hultgren[2]

Department of Molecular Microbiology, Box 8230 and [1]Department of Cell Biology and Physiology, Box 8228, Washington University School of Medicine, St Louis, MO 63110, USA
[2]Corresponding author

Communicated by S.Normark

Uropathogenic *Escherichia coli* produce heteropolymeric surface fibers called P pili, which present an adhesin at their tip that specifically recognizes globoside receptors on the host uroepithelium. The initial attachment step is thought to be essential for pathogenesis. P pili are composite fibers consisting of a thin tip fibrillum joined end to end to a rigid helical rod. Here we show that the ordered assembly of these structures requires the activity of two proteins that are minor components of the tip fibrillum, PapF and PapK. PapF is required for the correct presentation of the adhesin at the distal end of the tip fibrillum. PapK regulates the length of the tip fibrillum and joins it to the pilus rod. We propose that these subunits function as adaptors, by providing complementary surfaces to different substructures of the pilus and promoting their proper associations. In addition, the conversion of chaperone-subunit complexes into pili depends on PapF and PapK since a *papF*$^-$ *papK*$^-$ double mutation abolishes piliation. We suggest that in addition to the adaptor functions of PapF and PapK, they are also required to initiate the formation of tip fibrillae and pilus rods.

Key words: adaptor/adhesin presentation/initiator/pilus biogenesis/pyelonephritis

Introduction

Adhesion to host tissue receptors is a prerequisite for successful colonization by many Gram-negative pathogens. Attachment is mediated by bacterial surface adhesins, commonly associated with supramolecular structures called pili. These structures are often long complex heteropolymers that present adhesins away from the bacterial cell surface and its interfering lipopolysaccharides. Most uropathogenic strains of *Escherichia coli* produce P pili, which mediate binding to the globoseries of glycolipids. P pili are composed of six different subunit types, PapA, PapH, PapE, PapF, PapG and PapK. The assembly of these six subunit types into pilus fibers requires a periplasmic chaperone (Hultgren *et al.*, 1989; Lindberg *et al.*, 1989; Kuehn *et al.*, 1991) and an outer membrane protein called an usher (Norgren *et al.*, 1987; Dodson *et al.*, 1993) acting in concert to regulate the correct protein-protein interactions required for pilus assembly (for a recent review, see Hultgren *et al.*, 1991). P pili were recently shown to be composite fibers consisting of a long, stiff helical polymer joined end to end to a flexible thin fiber called a tip fibrillum (Kuehn *et al.*, 1992). The PapG adhesin that binds to Galα(1-4)Gal is present at the distal end of the tip fibrillae (Kuehn *et al.*, 1992). PapA is the major subunit that forms the bulk of the pilus, while PapE is the main constituent of the tip fibrillum (Kuehn *et al.*, 1992), and interestingly has been shown to be a fibronectin binding protein (Westerlund *et al.*, 1991). PapH was demonstrated to terminate the polymerization of PapAs and to anchor the pilus to the bacterial cell (Baga *et al.*, 1987). PapF was found to be a minor component of the pilus required for receptor binding (Lindberg *et al.*, 1987; Lund *et al.*, 1987), however, its role in pilus biogenesis has remained poorly understood. More recently, the gene coding for another pilin-like protein, PapK, was sequenced (Marklund *et al.*, 1992), but no function was attributed to it. PapD is a periplasmic chaperone that binds to subunit proteins as they emerge from the cytoplasmic membrane during translocation and shields their interactive surfaces from causing improper polymerization in the periplasm, thus preventing their aggregation and proteolytic degradation (Hultgren *et al.*, 1989; Kuehn *et al.*, 1991). The complexes are then targeted to an outer membrane assembly site consisting of the PapC usher. The usher has been suggested to act as a molecular doorkeeper which receives the subunit-chaperone complexes and incorporates the subunits into the architecturally distinct fibers (Dodson *et al.*, 1993).

Assembly of a large variety of pili in many different Gram-negative organisms requires periplasmic chaperones and outer membrane ushers that belong to the same families of proteins of which PapD and PapC, respectively, are the prototypes (Norgren *et al.*, 1987; Holmgren *et al.*, 1992; Dodson *et al.*, 1993). In addition, minor pilus proteins located at the tip or along intervals of the fimbriae have been proposed to be involved in pilus biogenesis (Klemm and Christiansen, 1987; Riegman *et al.*, 1988, 1990a; Oudega *et al.*, 1989; Simons *et al.*, 1990; Russel and Orndorff, 1992). Virtually nothing, however, is known of how the ordered assembly of these highly complex fibers proceeds to ensure the correct presentation of the adhesin making it able to bind specific eukaryotic receptors. Building the correct pilus architecture demands that each subunit be incorporated at the right time and position in the pilus. It has recently been suggested that PapC plays an essential role in this process, by modulating the ordered targeting of the various chaperone-subunit preassembly complexes to the assembly site (Dodson *et al.*, 1993). Also the relative concentrations of each subunit type in the periplasm are known to influence the assembly, as overproduction of PapH compared with PapA resulted in shorter pili (Baga *et al.*, 1987). Our present studies, however, indicate that the ordered assembly of the pilus fiber is mainly a function of the surface properties of the subunits themselves.

Here we report the details of the sequential

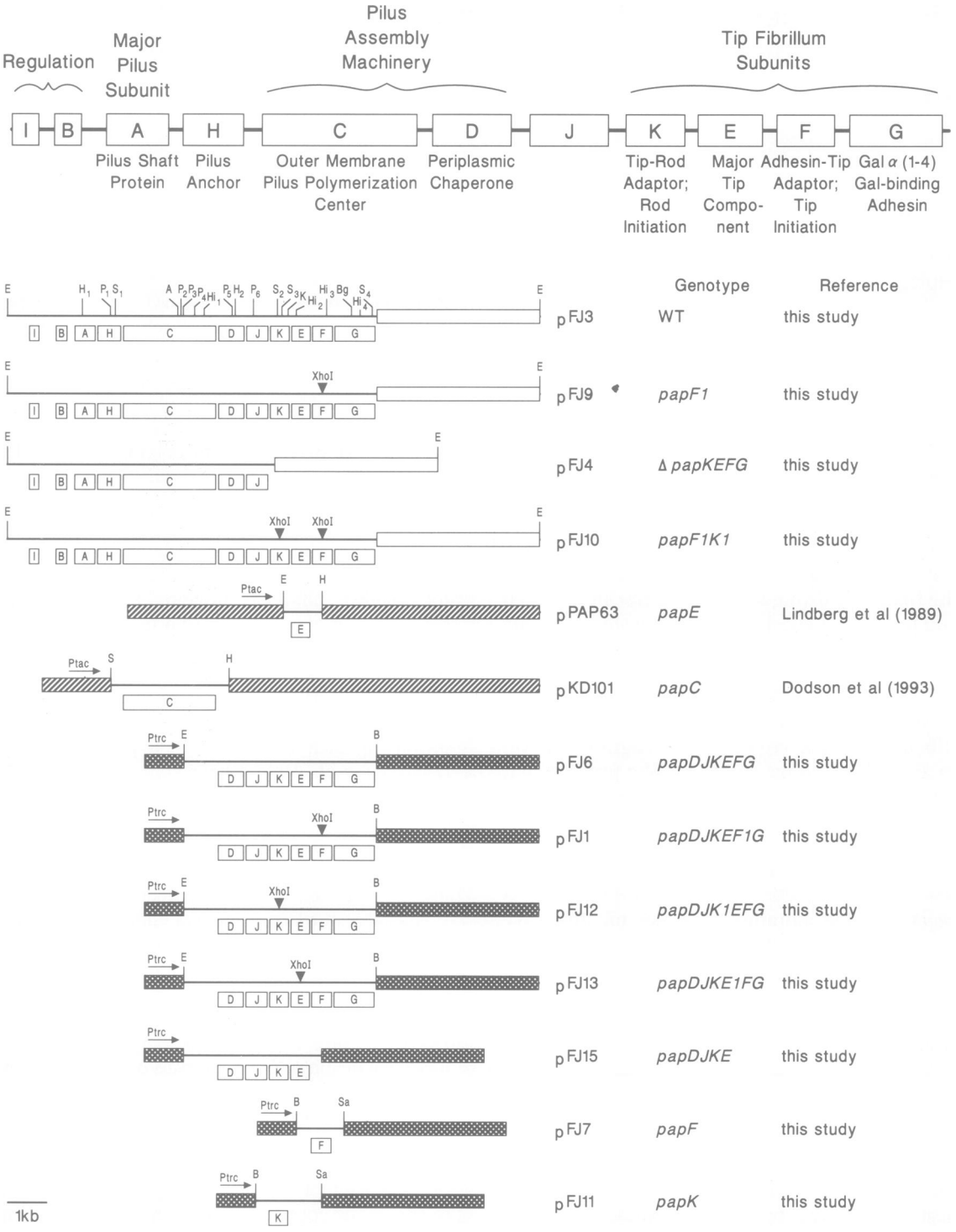

Fig. 1. Structure of the *pap* operon and plasmids used in this study. The functions of the different gene products are indicated. Open bars indicate the pACYC184 vector, hatched bars the pMMB91 vector and crossed bars the pTrc99A vector. The genetic lesions *papF1*, *papK1* and *papE1* result from the insertion of a *Xho*I linker at the indicated restriction sites, whereas various deletions lead to truncated versions of the operon (see genotype). Details of the construction of the various plasmids are given in Materials and methods. Restriction endonuclease sites are as follow: E, *Eco*RI; H, *Hin*dIII; P, *Pst*I; A, *Acc*I; Hi, *Hin*cII; K, *Kpn*I; S, *Sma*I; Sa, *Sal*I.

protein–protein interactions that lead to the ordered assembly and a precise architecture and composition of the P pilus. We suggest that complementary surfaces between subunits drive the process in conjunction with the assembly platform PapC. Specifically, PapF and PapK were shown to be minor components of the tip fibrillum and to play essential roles as initiators of polymerization and as adaptor proteins. PapF was shown to be required to initiate tip fibrillum assembly and to correctly present the PapG adhesin so that it could mediate receptor binding. The incorporation of PapK was found to terminate tip fibrillum growth and nucleate the formation of the pilus rod.

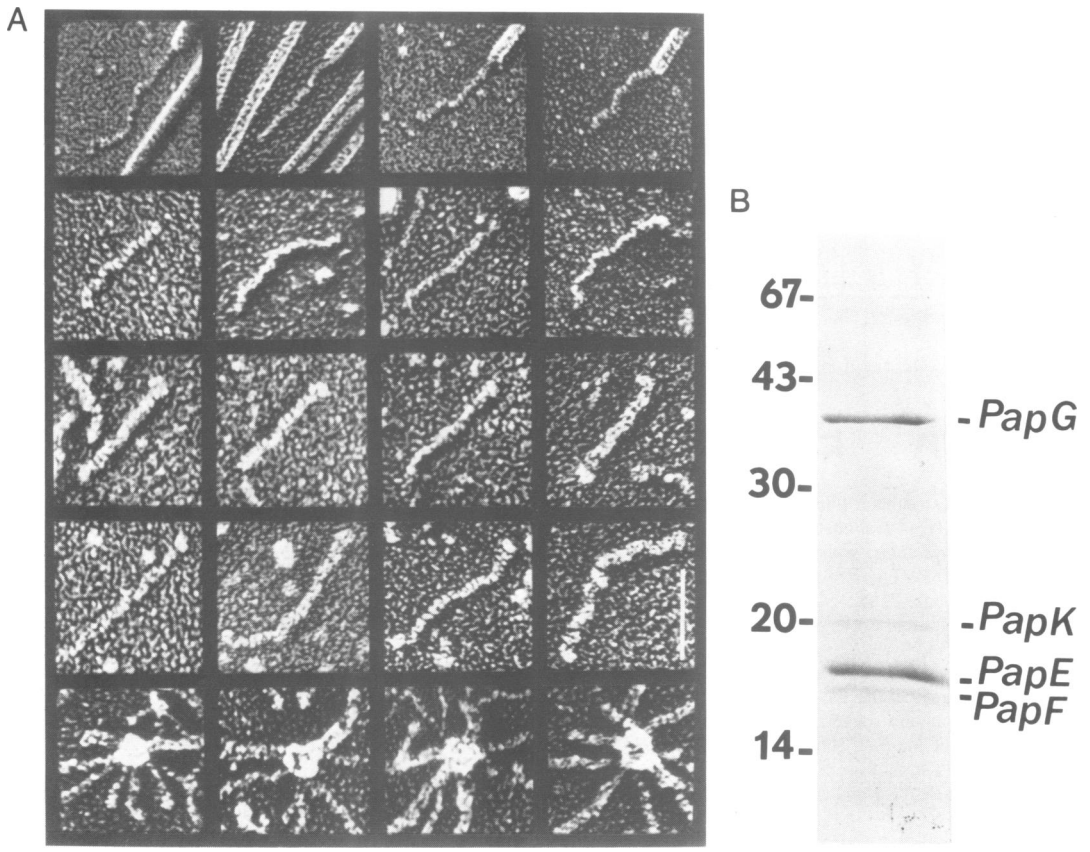

Fig. 2. Architecture and composition of adhesive tip fibrillae. **A.** Electron micrographs of pili and tip fibrillae: row 1, purified P pili showing flexible tip fibrillae at the distal ends of the rigid pilus rods; rows 2–5, affinity-purified tip fibrillae. In most cases the fibrillae seem to aggregate either laterally or by forming rosettes. The bar represents 0.05 μm. **B.** Affinity-purified tip fibrillae separated using 15% SDS–PAGE and Coomassie-stained. The identity of the protein bands was confirmed by amino-terminal sequencing following blotting onto polyvinylidene difluoride (PVDF) paper. Note that the purification of the tip fibrillae was dependent on PapG binding to the Galα(1–4)Gal sepharose. Copurification of the other subunits reflects their incorporation into the adhesive tip fibrillae.

Results

The tip fibrillum is a heteropolymeric structure

In the absence of the major PapA subunit no pilus rods are detected on the surface of the bacteria, yet they are still able to agglutinate human red blood cells (hRBC) (Uhlin *et al.*, 1985), most likely due to the assembly of adhesive tip fibrillae (Kuehn *et al.*, 1992). To define the composition of tip fibrillae, HB101 cells containing pKD101 that carried the *papC* gene under the control of an inducible *Ptac* promoter (Dodson *et al.*, 1993), were transformed with pFJ6 (*papDJKEFG*) (Figure 1). The simultaneous induction of the genes in both vectors led to the production of adhesive structures on the surface of the cells as determined by a high Galα(1–4)Gal-specific hemagglutination (HA) titer. Cells containing only one of these two plasmids were unable to bind human erythrocytes. The adhesive structures on the surface of the HB101/pFJ6,pKD101 cells were released by heating and purified by PapG-specific Galα(1–4)Gal affinity chromatography. Electron microscopy showed that the purified adhesive structures were tip fibrillae similar to those distally located on whole pili (Figure 2A). Tip fibrillae were also seen on the surface of whole cells by electron microscopy (not shown). They were found to be composed of four proteins by SDS–PAGE (Figure 2B). Amino-terminal sequencing of the four proteins identified them as PapE, PapK, PapF and PapG (not shown). Although PapG and PapE seemingly stained with similar relative intensities by Coomassie blue, the relative amounts of amino acid residues released from the amino-terminal sequencing of each protein band argued that PapE was at least 5-fold more abundant than any of the other tip fibrillar proteins. This is in agreement with previous studies that have shown that most of the tip fibrillum is composed of repeating subunits of PapE (Kuehn *et al.*, 1992). In addition, PapE has also been shown to be the second most abundant protein in the pilus next to PapA (Kuehn *et al.*, 1992).

PapF is required to link the PapG adhesin to the tip fibrillum

To define which proteins are required for the formation of tip fibers, expression of tip fibrillae was analyzed in the *papF1*, *papE1* and *papK1* mutants using the following combinations: HB101/pKD101, pFJ1 (*papC*, *papDJKEF1G*: F^-), HB101/pKD101, pFJ12 (*papC*, *papDJK1EFG*: K^-) and HB101/pKD101, pFJ13 (*papC*, *papDJKE1FG*: E^-). Tip fibrillae preparations from the wild type (WT) and each of the mutant strains were subjected to PapG-specific Galα(1–4)Gal affinity chromatography. This experiment investigated the order of the four subunit types in the tip fibrillum and their roles in joining each subunit type to another. PapF, PapK and PapE were copurified with PapG

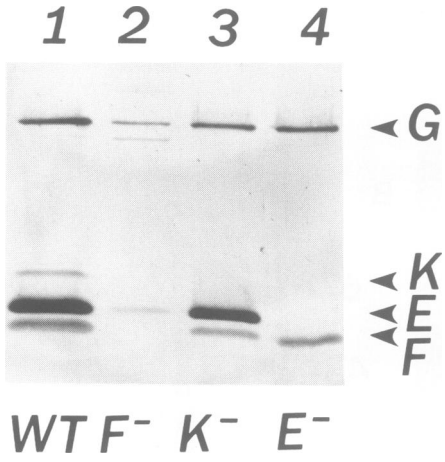

Fig. 3. Complementary surfaces on each fibrillar subunit type. Tip fibrillae were purified by Galα(1−4)Gal chromatography from cells missing one of the tip fibrillar proteins, with the following plasmid combinations: pKD101 + pFJ6 (WT control, lane 1), pKD101 + pFJ1 (F^-, lane 2), pKD101 + pFJ12 (K^-, lane 3) and pKD101 + pFJ13 (E^-, lane 4). The preparations were separated by using 15% SDS−PAGE, transferred to PVDF, and the Western blots were developed using anti-tip fibrillar antiserum. Very little PapE is detected in association with adhesive PapG in the F^- tip fibrillae. The presence of a PapG truncate in the F^- mutant suggests that PapG is more prone to degradation in the absence of PapF. It should be noted that the antiserum used for this analysis was raised against purified whole tip fibrillae and recognizes PapE, PapF, PapK and PapG with different titers.

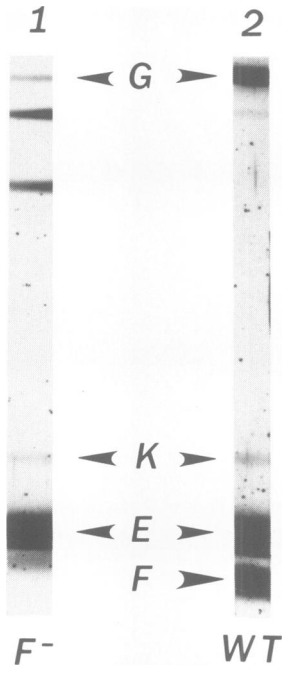

Fig. 4. Tip fibrillae from WT and F^- strains. Tip fibrillae from the WT strain (pKD101 + pFJ6, lane 1) and from the *papF1* strain (pKD101 + pFJ1, lane 2) were purified by a centrifugation on a sucrose gradient, eliminating the dependence on PapG for purification. The tip fibrillae-containing fractions were separated by 15% SDS−PAGE and tranferred on PVDF paper. The Western blots were developed using anti-tip fibrillar antiserum. Note that PapE fibers are formed in F^- tip fibrillae. Significantly more tip fibrillae were obtained from the WT strain, but the concentrations of the two preparations were adjusted so that approximately equal amounts of PapE were loaded in both cases. Note that similar amounts of PapK are found in both preparations, but significantly less PapG is present in the F^- tip fibrillae. The bands under PapG in the F^- preparation are thought to be PapG truncates. The inability to significantly copurify PapE with PapG by Galα(1−4)Gal affinity chromatography (see Figure 3) argues that PapF is the adaptor between PapG and PapE.

in WT tip fibrillae, demonstrating that they are all joined to one another to make up the fiber (Figure 3, lane 1). In the absence of PapF the amount of PapG detected by Galα(1−4)Gal was greatly reduced (Figure 3, lane 2). In addition, PapE and PapK no longer copurified with PapG in significant amounts arguing that in the absence of PapF, PapG is not correctly joined to the tip fibrillum (Figure 3, lane 2). PapF most likely links PapG to PapE and not PapK, since in the absence of PapE, only PapF copurified with PapG and not PapK (Figure 3, lane 4). These results can best be explained if PapE is positioned between PapF and PapK. In support of this order was the finding that both PapF and PapE were copurified with PapG in the absence of PapK (Figure 3, lane 3). The E^- cells were virtually HA-negative (titer: 2^1-2^2), which was in agreement with previous results obtained with a *papA*$^-$*papE*$^-$ double mutant (Lindberg *et al.*, 1984). The K^- cells had an HA titer slightly lower than that of the WT (2^4-2^5 versus 2^6-2^7). Interestingly, the F^- cells were HA-negative.

The inability to purify significant amounts of PapE with PapG from the F^- strain could be due to the lack of a complementary surface between PapG and PapE. Alternatively it is possible that in the absence of PapF, PapE subunits do not assemble into fibers. To distinguish between those possibilities, F^- tip fibrillae were purified on a sucrose gradient, eliminating the requirement of a functional PapG adhesin for purification of the putative fiber. PapE oligomers migrated at the same position in the gradient (~15% sucrose) as WT tip fibrillae, demonstrating that PapE subunits assemble into fibrillae in the absence of PapF. PapK was found incorporated in the F^- fibrillae in seemingly normal amounts, but significantly less PapG was associated with the PapE oligomers than in the WT tip fibrillae purified in the same way (Figure 4). In addition, PapG truncated bands were also present in the F^- sucrose gradient fractions (Figure 4). The decreased association of PapG with PapE and the presence of truncates argue that PapF serves as an adaptor that is required to link PapG in a functional manner to the PapE tip fibrillum. This conclusion is also supported by the HA-negative phenotype of the *papF1* mutation.

Subunit interactions in the periplasm reflect interactions occurring for tip formation

In the absence of the outer membrane usher PapC, no pili are assembled on the surface of the cells, and subunits are found in the periplasm as preassembly complexes with the chaperone (Norgren *et al.*, 1987). Some association has been detected between subunits in the periplasm in the K88 pilus system (Mooi *et al.*, 1983). The interactions in the periplasm of different subunit types with the PapG−PapD complex were tested in the *pap* system by expressing the genes encoded by pFJ1 (*papDJKEF1G*: F^-), pFJ6 (*papDJKEFG*: WT), pFJ12 (*papDJK1EFG*: K^-) or pFJ13 (*papDJKE1FG*: E^-) in the absence of the outer membrane protein PapC. Periplasmic extracts were obtained from the four strains and the adhesin−chaperone preassembly complexes were affinity-purified using PapG-specific Galα(1−4)Gal chromatography to investigate whether other

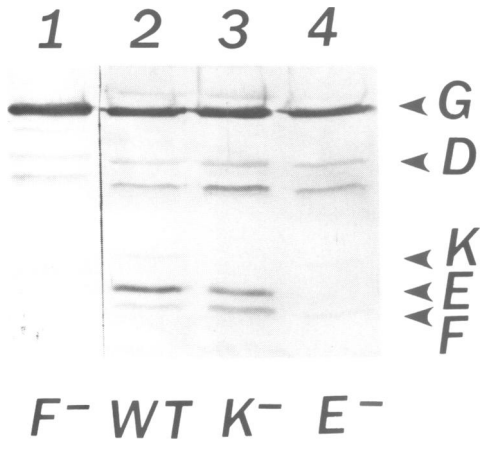

Fig. 5. Periplasmic complexes from several mutant strains. PapG-containing chaperone–subunits complexes were purified by PapG-specific Galα(1–4)Gal affinity chromatography from periplasmic extracts prepared from strains expressing pFJ1 (F^-, lane 1), pFJ6 (WT, lane 2), pFJ12 (K^-, lane 3) and pFJ13 (E^-, lane 4) in the absence of PapC. The complexes were separated by 15% SDS–PAGE. The Western blots were developed using anti-tip fibrillar antiserum (which slightly recognizes PapD as well). The protein band under PapD was reported to be a PapG truncate (Hultgren *et al.*, 1989).

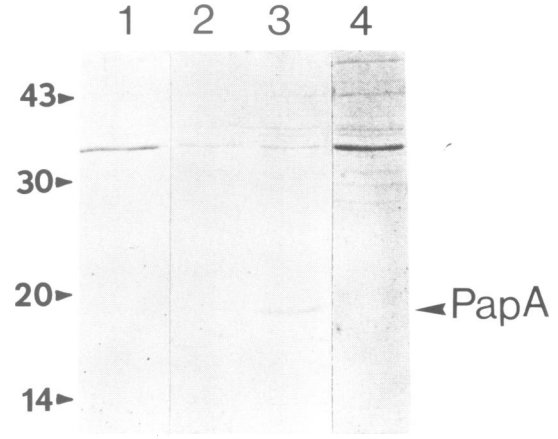

Fig. 6. PapK initiates pilus rod formation. Pili preparations were obtained from strains carrying pFJ4 (*papIBAHCDJ*: Tip^-) with the control plasmid pTrc99A (lane 1) or complemented *in trans* with pFJ7 (*papF*, lane 2), pFJ11 (*papK*, lane 3) or pPAP63 (*papE*, lane 4). Samples obtained from similar amounts of cells were boiled in loading buffer containing 4 M urea to dissociate the pili and separated using 15% SDS–PAGE. After Coomassie staining, a PapA band can only be detected from the strain producing PapK (lane 3), suggesting that only PapK is able to replace the entire tip fibrillum to initiate pilus rod formation.

Table I. Comparison of F^- and F^+ piliated strains: HA titers and quantification of pilus antigen by ELISA

Plasmids	pFJ3	pFJ9	pFJ9 + pTrc99A	pFJ9 + pFJ7
Phenotype	WT	F^-	F^-	WT
HA titer[a]	32–64	0	0	64
ELISA αPapA[b]	500	100	100	400
αTips[b]	800	100	100	500

[a]Highest dilution of cell suspension yielding detectable HA; '0' represents no detectable HA at any dilution.
[b]Relative amounts of antigen detected (control = 100).

subunit types were associated within this complex. In the periplasm of the WT clone, small amounts of PapE, PapK and PapF coeluted with the PapG–PapD complex (Figure 5). The identities of PapG, PapK and PapE were confirmed by amino-terminal sequencing. In the K^- and E^- periplasmic extracts, the elution profiles were identical to the wild type except for the absence of PapK and PapE, respectively. In the F^- periplasmic extract, however, hardly any PapE or PapK coeluted with the PapD–PapG complexes, virtually mimicking the linkage order found in the tip fibrillum.

These multiple subunit associations in the periplasmic space most likely result from the high concentrations of the preassembly complexes in the periplasm in the absence of the outer membrane usher PapC, and it is not known whether they represent intermediates in the assembly of pili. Nevertheless, the pilus subunits qualitatively associated with one another in the same fashion as they did in the final fibrillar structure. These data corroborated the observation that adhesive PapG was virtually not linked to PapE in the absence of PapF and strongly support the hypothesis that PapF is a necessary adaptor between the PapG adhesin and the PapE oligomer.

PapF affects pilus rod assembly

Cells containing the operon with a linker insertion in *papF* (pFJ9) were unable to agglutinate hRBC and produced at least 5-fold fewer pili than their WT counterparts, as determined by ELISA on purified pili (Table I). *PapF* cloned on the compatible pFJ7 plasmid was tested for its ability to complement the *papF1* lesion on pFJ9. Transcomplementation with *papF* restored a high HA titer and a WT level of piliation as determined by ELISA using anti-pilus and anti-tip fibrillar antisera (Table I). These data argued that in addition to linking PapG to the PapE fibrillum, PapF also plays a role in the polymerization of the pilus.

The role of PapF as an initiator of pilus formation was further investigated. Tip fibrillar formation was analyzed in HB101 cells where either pFJ15 (*papDJKE*: F^-G^-), pFJ6 (*papDJKEFG*: WT) or pFJ1 (*papDJKEF1G*: F^-) were expressed *in trans* with pKD101 (*papC*). Tip fibrillae were semi-purified from each strain by ammonium sulfate precipitation and quantified by either ELISA or by comparing the relative intensities of PapE bands present in Western blots stained by anti-tip fibrillar antisera. Using both methods, an intermediate quantity of tip fibrillum proteins was found in the F^-G^- strain, as compared with F^- and WT (not shown). This suggested that the lower level of piliation obtained in a F^- strain could be partially relieved by simultaneously removing *papG* from the operon.

PapK, but not PapF, can initiate PapA polymerization into the pilus rod

Expression of *papIBAHCDJ* from HB101/pFJ4 (Tip^-) cells containing the pTrc99A vector as a control, resulted in a non-piliated phenotype, as monitored by ELISA and SDS–PAGE, demonstrating that pilus rod formation does not take place in the absence of the tip proteins (Figure 6, lane 1). In an attempt to restore a piliated phenotype, HB101/pFJ4 (Tip^-) was complemented *in trans* with either pPAP63 (PapE overproducer: E^+, Lindberg *et al.*, 1989), pFJ7 (PapF overproducer: F^+) or pFJ11 (PapK

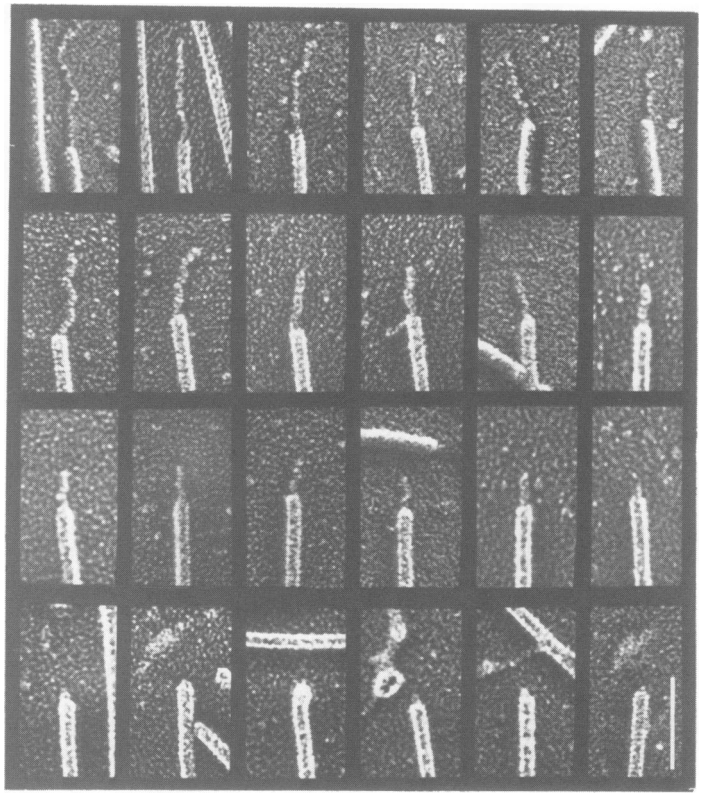

Fig. 7. PapK regulates tip fibrillum length. Row 1 shows pili preparations from a strain carrying the WT *pap* operon on pFJ3; rows 2 and 3 show pili purified from a strain where PapK was overproduced under the *tac* promoter, using pFJ3 + pFJ11 (*papK*). Note that overproducing PapK shifts the distribution of tip fibrillar lengths so that most are now much shorter than the wild type structures. Row 4 shows pilus rods nucleated by the production of PapK expressed on pFJ11 (*papK*) *in trans* with pFJ4 (*papIBAHCDJ*: Tip$^-$). Only a small knob, that may represent PapK, can be seen in some instances. The bar represents 0.05 μm.

overproducer: K$^+$). Neither of the first two combinations was able to restore piliation, as determined by the lack of a PapA band in Coomassie-stained SDS−PAGE of pili preparations from these strains (Figure 6, lanes 2 and 4) and by the lack of reactivity of the cells or pili preparations to anti-pilus antiserum in an ELISA (not shown). However, Western blotting of the pili preparations from the three strains Tip$^-$, Tip$^-$F$^+$ and Tip$^-$E$^+$, using anti-pilus antiserum, revealed faint PapA bands (not shown). Complementation of HB101/pFJ4 (Tip$^-$) with pFJ11 (PapK overproducer: K$^+$) induced the formation of pili by 20-fold more than in cells carrying pFJ4,pTrc99A (vector alone), as determined by ELISA using anti-pilus antiserum (not shown) and Coomassie-stained SDS−PAGE on pili preparations (Figure 6, lane 3). However, the level of piliation obtained with the HB101/pFJ4,pFJ11 (Tip$^-$ K$^+$) strain was at least 10-fold lower than that of a WT strain.

Electron microscopy performed on purified pili from HB101/pFJ4,pFJ11 (Tip$^-$K$^+$) confirmed the absence of a fibrillar structure at the tip of these pili, unlike wild type pili, in which long fibrous tips are seen (Figure 7, row 1). A very short knob was detected at the distal end of the pilus rod of some Tip$^-$K$^+$ pili, which is presumably composed of PapK (Figure 7, row 4). These results suggested that PapK might imperfectly substitute for whole tip fibrillae as a nucleator of PapA polymerization.

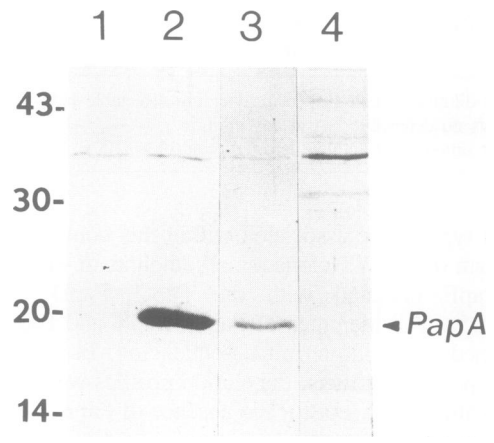

Fig. 8. PapF or PapK is required for pilus assembly. Pili preparations were obtained from HB101 strains carrying the following plasmid combinations: pFJ10 + pTrc99A (F$^-$K$^-$, lane 1), pFJ10 + pFJ7 (F$^-$K$^-$ transcomplemented with *papF*, lane 2), pFJ10 + pFJ11 (F$^-$K$^-$ transcomplemented with *papK*, lane 3) and pFJ10 + pPAP63 (F$^-$K$^-$ transcomplemented with *papE*, lane 4). Samples obtained from similar amounts of cells were boiled in 4 M urea loading buffer and separated using 15% SDS−PAGE. No PapA band can be detected in the pili preparation from the double mutant after Coomassie staining of the gel, nor when it is transcomplemented by *papE*, whereas transcomplementation with *papF* or *papK* fully or partly restores piliation, respectively.

PapK regulates the length of the tip fibrillum

Interestingly, tip fibrillae from a *papK1* strain were previously shown to be significantly longer than WT fibers, suggesting that PapK may regulate the length of the tip fibrillum (Kuehn *et al.*, 1992). The role of PapK in terminating the growth of the tip fibrillum was investigated by examining the effect of overproducing PapK, in the presence of the WT *pap* operon, on tip fibrillum length.

Table II. Complementation of the double F^-K^- mutant with *papF* or *papK*

Plasmids	pFJ10 + pTrc99A	pFJ10 + pFJ11	pFJ10 + pFJ7
Phenotype	F^-K^-	F^-	K^-
Ha titer	0	0	32
ELISA αPapA (pili)[a]	100	1200	>10 000
ELISA αPapA (cells)[b]	100	2000	>4000

[a]ELISA performed on pili preparations.
[b]ELISA performed on piliated cells.

Electron microscopy of the purified pili revealed that overproduction of PapK resulted in a significant shift of the distribution of the lengths of the K^+ tip fibrillae when compared with WT, so that most were now much shorter than the wild type structures (Figure 7). The average length of the K^+ tip fibrillae was 30 ± 19 nm (n = 79), which was found to be significantly shorter than the average length of WT tip fibrillae, 43 ± 31nm (n = 123). The best interpretation of these results is that the incorporation of PapK terminates growth of the tip fibrillum.

The F^-K^- double mutant cannot assemble pili

The reduction, but not abolition, of piliation caused by a linker insertion in *papF* suggested that PapF triggers an initial event required for pilus assembly, but also implied that other protein(s) in the operon are able to do so in the absence of PapF. HB101 cells containing pFJ10, which carried the *papF1papK1* double mutant (F^-K^-), were found to be virtually non-piliated, as determined by ELISA and SDS–PAGE of purified pili preparations (Figure 8, lane 1). The piliation phenotype could be rescued by overproducing *in trans* either PapF using pFJ7 or PapK using pFJ11 (Figure 8, lanes 2 and 3), but only in the first case did the cells produce a high HA titer (2^5–2^6). Transcomplementation of the F^-K^- double mutant with *papF* resulted in the production of significantly more pili than when complemented with *papK*, as determined by using anti-pilus antiserum in ELISA assays on whole cells and pili preparations (Table II). Electron microscopic examination of the few available pili from the F^-K^- double mutant suggested that they were devoid of tip fibrillae, arguing that either PapF or PapK was necessary to initiate tip fibrillum formation (not shown).

We tested whether overexpression of PapE *in trans* using pPAP63 (E^+) in the presence of pFJ10 (*paF1papK1*: F^-K^-) could restore the presence of tip fibrillae or composite pilus fibers. No PapA band was detected by Coomassie-stained SDS–PAGE of pili preparations of the $F^-K^-E^+$ strain (Figure 8, lane 4). In addition, PapE could not be detected by Western blotting using anti-tip fibrillar antiserum. Similarly, no tip fibrillae were detected in the supernatant of the $F^-K^-E^+$ strain as shown by the lack of a PapE band by Western blotting using anti-tip fibrillar antiserum on sucrose gradient purified tip fibrillar preparations from the concentrated supernatant (not shown), in contrast to what had been observed with the F^- strain using a similar procedure. Electron microscopy showed that no tip fibrillae were present on any of the very few pili available (not shown). These data suggest that the initiation of the assembly of a tip fibrillum requires PapF or PapK.

Discussion

The assembly of pili by Gram-negative bacteria seems to be a highly controlled process, ensuring that every pilus has virtually the same composition and structure. In addition, the extracellular location of these appendages requires a high resistance to mechanical forces. Indeed, the quaternary structure of pili was shown to be extremely resistant to dissociation (Salit and Gotschlik, 1977; Mc Michael and Ou, 1979; Eshdat *et al.*, 1981; R.Striker and S.Hultgren, unpublished observations). Our results suggest that the correct incorporation of the various components into the pilus is dictated by stereochemical fits between the complementary surfaces on each subunit type. The composite structure of the P pilus joins a rigid helicoidal polymer (Gong and Makowski, 1992) to a flexible tip fiber, allowing for the efficient presentation of the adhesin with maximum steric freedom (Kuehn *et al.*, 1992). Two minor pilus components, PapF and PapK, are crucial to ensure that the assembly of the adhesive tip fibrillum precedes that of the pilus rod and that the substructures of the pilus are firmly connected. PapF was shown to be an adaptor protein that is required to link the PapG adhesin to the distal end of the tip fibrillum. In addition in an F^- mutant, only ~20% of the WT piliation level is obtained, arguing that the PapF adaptor protein also has an initiator function, as previously suggested (Lindberg *et al.*, 1987). Interestingly, PapK also has a dual initiator/adaptor function. The incorporation of PapK terminates the growth of the tip fibrillum and nucleates the formation of the pilus rod. The P pilus is composed of two distinct structures and this requires two specialized subunits, PapF and PapK, to initiate the assembly of each structure subtype and join each structural element within the pilus.

The inability of the F^-K^- double mutant to form pilus rods or tip fibrillae demonstrated that the presence of subunits known to form fibers, PapA and PapE, together with the assembly machinery, was not sufficient to initiate polymerization. The observed phenotype was reminiscent of a $PapC^-$ mutant, which also resulted in a non-piliated phenotype. The inability to form fibers in either the C^- or the F^-K^- backgrounds is presumably due to a block in the chaperone uncapping mechanism, which exposes polymerization surfaces on the subunits driving their assembly, and is thought to be mediated by PapC (Hultgren *et al.*, 1991). The data argue that PapF or PapK are involved in triggering the chaperone uncapping mechanism and can best be explained by proposing the following cascade of protein–protein interactions (Figure 9). After the targeting of the PapD–PapG complex to PapC, the PapD–PapF complex interacts with the ternary PapC–PapD–PapG complex to trigger the uncapping of PapD from PapG. The PapG adhesin is joined to the distal end of the tip fibrillum via PapF and uncapping of PapD allows the PapE subunits to polymerize into the tip fibrillum. The relative concentrations of the PapD–PapE and PapD–PapK complexes in the periplasm, as well as their respective affinities for the PapC site occupied by the nascent oligomer, determines the length of the tip fibrillum. The incorporation of a PapK subunit into the tip fibrillum terminates its growth and nucleates the formation of the pilus rod. The affinity of PapD–PapA complexes for a PapC site already occupied by a tip fibrillum terminated with PapK initiates rod polymerization. Interestingly, PapA–PapD complexes are not thought to be targeted to empty PapC sites (Dodson

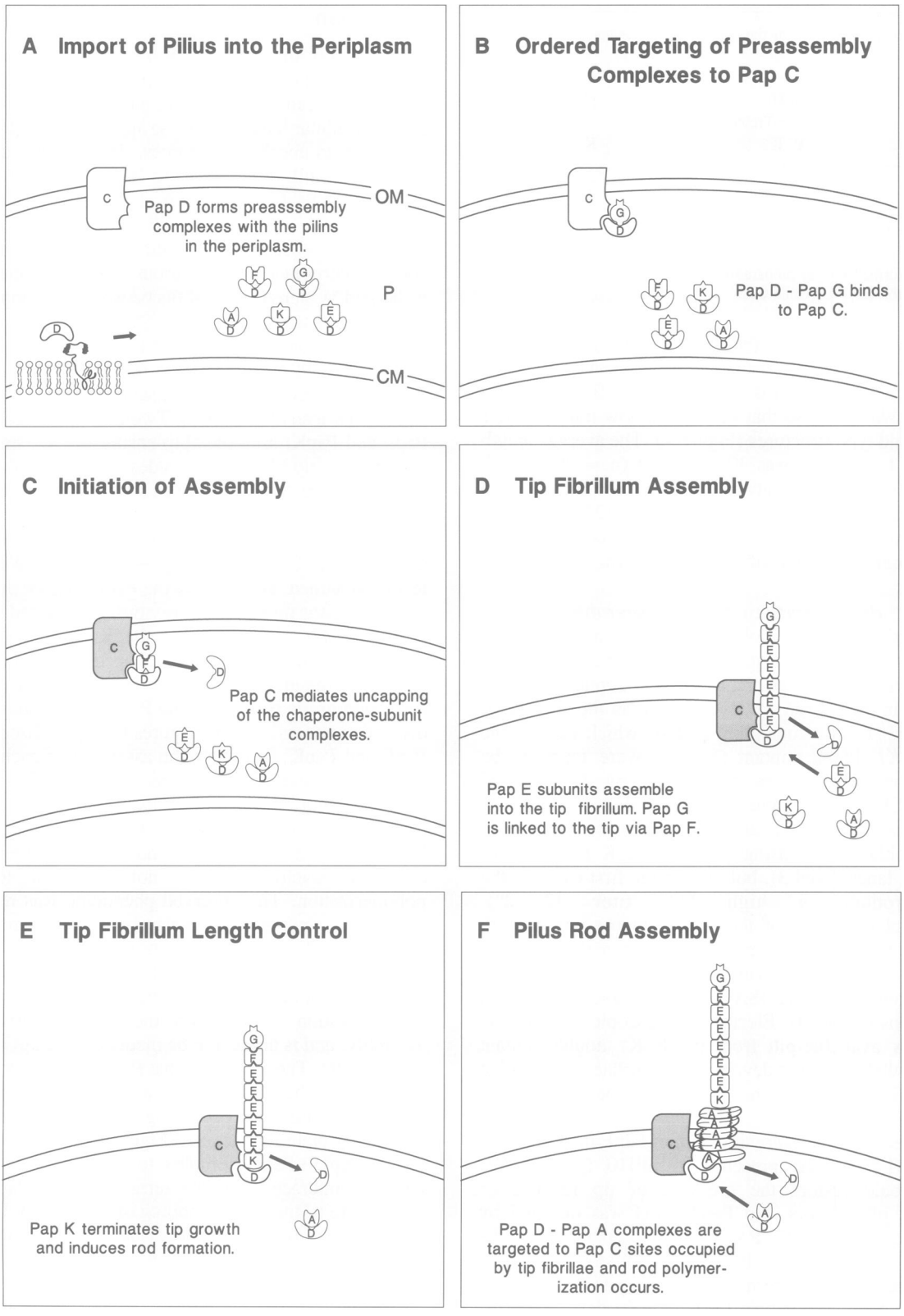

Fig. 9. Model for the assembly of P pili. The details are given in the text.

et al., 1993), which is a mechanism to ensure that every pilus rod is joined end to end to an adhesive tip fibrillum. The polymerization of PapAs into a helical structure then proceeds until a PapH subunit is incorporated and terminates the growth of the pilus (Baga *et al.*, 1987). In the WT strain, the growing fiber presented at each step in the PapC site allows the correct incorporation of the next subunit. The proper succession of these steps is driven by stereochemical fits between the complementary surfaces of the different subunit types and this mechanism ensures the correct composition of the P pilus *in vivo*.

In an F^- strain, initiation of tip fibrillum polymerization at the PapC sites occupied by PapD–PapG complexes occurs inefficiently due to the absence of PapF to link PapG to

PapE. The low level of tip fibrillum assembly in a F^- strain is partially relieved by deleting *papG* (F^-G^- double mutant). This supports our model in which PapC sites are occupied by PapD–PapG complexes until PapF initiates tip fibrillum assembly and links PapG to the tip. In agreement with these findings is the observation that the expression of *papF* seems very low *in vivo* (unpublished observations). Keeping the concentration of PapF equal to or below that of PapG may be part of a mechanism to prevent initiation of pili devoid of an adhesin. A correlation between the level of adhesion and the initiation of polymerization has been reported in other pilus systems as well (Riegman *et al.*, 1988; Schmoll *et al.*, 1989; Schifferli *et al.*, 1991).

PapK regulates the length of the tip fibrillum. Overproduction of PapK shifted the distribution of tip fibrillar lengths so that most were significantly shorter than wild type. In the K^+ strain, the increased ratio of PapD–PapK to PapD–PapE complexes in the periplasm probably increased the frequency by which a PapK subunit was incorporated, thereby prematurely interrupting the growth of the tip fibrillum. This hypothesis was supported by the finding that in a K^- strain, tip fibrillae were significantly longer (Kuehn *et al.*, 1992). Apparently PapA subunits were able to associate with tip fibrillae terminated by PapE, but with a low efficiency, resulting in the incorporation of a larger number of PapE subunits before PapA polymerization was initiated. In the absence of PapK, the HA titer was generally lower than WT and according to electron microscopy, more pili were devoid of tip fibrillae (M.Kuehn and S.Hultgren, unpublished observations). PapK probably provides the proper linkage between the linear tip fibrillum and the helical pilus rod, thereby avoiding the shedding of the adhesive moiety of the pilus.

Deletion of the four tip fibrillar genes abolished the ability of the cells to produce pili. Only the expression of *papK in trans* was able to initiate rod polymerization without the rest of the tip fiber. In an F^- mutant, chaperone uncapping at the outer membrane assembly site is probably triggered by PapK, allowing PapEs to polymerize into a tip fibrillum. This suggests that both PapF and PapK are capable of acting as initiators of pilus polymerization, albeit by an unknown mechanism. The location of PapF in the tip fibrillum is suggested by its adaptor function and the location of PapK by its role in regulating tip fibrillar length and nucleating pilus rod assembly. The dependence on either PapF or PapK for pilus assembly and the ability of PapF and PapK to apparently substitute for one another in the initiation function, could indicate that both PapF and PapK may be present at both ends of the PapE fibrillae. However, we favor the model presented in Figure 9 since only PapF can link PapG to the PapE fibrillum and only PapK by itself can nucleate the formation of pilus rods. Furthermore, PapK is not linked to the PapG–PapF moiety in the absence of PapE as determined by Galα(1–4)Gal chromatography.

In the absence of both PapF and PapK, very few pili could be detected by electron microscopy. Similarly, low levels of piliation were reported in the absence of the outer membrane protein (Riegman *et al.*, 1990b). We suggest that there exists an alternative biosynthetic pathway that bypasses the strict requirement for the minor subunits, most likely due to high concentrations of preassembly complexes in the periplasmic space and the strong tendency of PapA subunits to self-polymerize. This 'unprimed' assembly process is probably energetically unfavorable, making the alternative pathway extremely infrequent.

The work presented here reveals both singular features and general principles for pilus assembly in Gram-negative bacteria. To date, only P pili have been reported to be composed of two different structures, but no other pili have been examined under electron microscopy at such high resolution. Several reports about different pili systems indicate that minor subunits are involved in initiation of assembly (Klemm and Christiansen, 1987; Simons *et al.*, 1990; Schifferli *et al.*, 1991; Russel and Orndorff, 1992) and also suggest that preassembly periplasmic complexes associate with the outer membrane usher to activate polymerization (Mooi *et al.*, 1983; Oudega *et al.*, 1989; Riegman *et al.*, 1990b). Many Gram-negative bacteria assemble adhesive pili as an efficient means of binding to specific eukaryotic receptors. This initial binding event is often crucial to pathogenesis. In spite of variations related to the particular epithelium colonized, pilus assembly in Gram-negative bacteria requires proteins with similar functions and structures (Holmgren *et al.*, 1992; Dodson *et al.*, 1993). Our present work has unveiled for the first time the role of tip fibrillar proteins that are required for pilus formation. Minor variations on this general theme will most likely be discovered as other pili systems are dissected at a similar level of molecular resolution.

Materials and methods

Plasmid construction

pFJ6 was constructed by cloning the carboxy-terminal part of the operon, comprised of *papDJKEFG* genes (thus excluding the main subunit *papA* gene), excised from pPAP58 (Hultgren *et al.*, 1989) into the high copy number vector pTrc99A (Pharmacia), under the control of the strong inducible *Ptrc* promoter (see Figure 1).

pFJ1 is similar to pFJ6 except for a linker insertion in *papF*. It was obtained by cloning the *Bam*HI–*Acc*I fragment (*papDJKEF1G*) from pPAP14 (Lindberg *et al.*, 1984) into the *Bam*HI-blunted *Eco*RI sites of the pTrc99A linker. pFJ12 (*papDJK1EFG*) and pFJ13 (*papDJKE1FG*) were obtained through the replacement of the *Eag*I–*Bam*HI fragment of pFJ6 by the similar fragments from pPAP42 (*papK1*) (Lindberg, 1987) and pPAP15 (*papE1*) (Lindberg *et al.*, 1984).

pFJ3 (WT) and pFJ9 (F^-) were constructed by cloning the wild type operon and its F^- version containing an out-of-frame linker in the *papF* gene, as *Eco*RI-blunted *Bam*HI fragments excised from pPAP5 and pPAP14 respectively (Lindberg *et al.*, 1984), into the *Eco*RI–*Sca*I sites of pACYC184.

pFJ4 encoded the *pap* operon without any of the tip proteins (Δ*papKEFG*) and was constructed by cloning the *Eco*RI-blunted-*Xho*I fragment from pPAP42-blunted- (Lindberg, 1987) in the *Eco*RI–*Sca*I sites of pACYC184.

pFJ10 encodes the *pap* operon with the double *papF1papK1* mutation and was constructed by replacing the *Kpn*I–*Eco*RI fragment of pFJ9 (*papF1*) with the same fragment from pPAP42 (*papK1*).

pFJ15 (*papDJKEF1DG*) was obtained from pFJ1 by digestion with *Xho*I (inside the linker inactivating *papF*) and *Sal*I (in the polylinker of the vector) and religation.

pFJ7 encodes *papF* and was obtained as a PCR-amplified fragment. Two oligonucleotides 5′-CGGGATCCTTTCTGTACCGCTCTCC-3′ and 5′-C-CGCGTCGACACTTCCGTAATTACAGT-3′, which were complementary to sequences on each side of *papF* in the operon but with *Bam*HI and *Sal*I sites added at the extremities, were used in a PCR reaction using pPAP58 (Hultgren *et al.*, 1989) as a template (24 cycles of 1 min at 94°C, 2 min at 45°C and 2 min at 72°C). The amplified fragment was digested at the extremities with *Bam*HI and *Sal*I, cloned in the polylinker of pTrc99A and completely sequenced using internal primers and a protocol for double strand sequencing (Zhang *et al.*, 1988).

The cloning of *papK* was performed similarly to that of *papF* to give pFJ11. The oligonucleotides 5′-CGGCGTCGACCCCCAGCATTACCG-3′ and 5′-GCGGATCCGGCCATGCTGCG-3′ were designed to hybridize on either side of *papK* in pPAP58 and to contain *Bam*HI and *Sal*I sites at their

extremities. That portion of DNA was amplified as described above and the amplified DNA fragment was digested, recloned and sequenced in the same manner as described for pFJ7.

Purification of tip fibrillae

HB101 cells containing both pFJ6 (*papDJKEFG*) and pKD101 (*papC*) were grown until the absorbance of the culture at 600 nm reaches 0.8 in Luria Broth medium containing 50 mg/l carbenicillin and 50 mg/l kanamycin. At this point, 1 mM isopropylthiogalactoside (IPTG) was added to induce expression of all the genes and the culture was grown for two more hours. Cells were spun down, washed once in phosphate buffered saline (PBS), resuspended in 0.5 mM Tris and 75 mM NaCl (pH 8) and heated for 30 min at 65°C to extract fimbriae. After pelleting the defimbriated cells and cell debris by two successive centrifugations (8000 *g* for 10 min and 27 000 *g* for 30 min), tip fibrillae present in the supernatant were precipitated using $(NH_4)_2SO_4$ at 50% saturation. Tip fibrillae were then affinity-purified using Galα(1−4)−Sepharose in a similar manner as the PapD−PapG preassembly complex was purified (Hultgren *et al.*, 1989). Various mutant tip fibrillae were obtained by combining pKD101 (*papC*) with pFJ1 (*papDJKEF1G*: F^-), pFJ12 (*papDJK1EFG*: K^-), pFJ13 (*papDJKE1FG*: E^-) or pFJ15 (*papDJKEF1*ΔG: F^-G^-) and purified as described above unless otherwise stated.

Sucrose gradient centrifugation

A discontinuous 5 ml 10, 15, 20 and 25% sucrose gradient in 20 mM Tris (pH 7.5) was poured in Ultra Clear TM Beckman centrifuge tubes and left overnight at 4°C. A 200−300 μl sample was carefully loaded on top of the gradient and spun at 40000 r.p.m. in a SW 50.1 rotor for 4 h at 4°C. Centrifugation was stopped without brakes. 250 μl fractions were collected from the bottom of the tube and analyzed by Western blotting after separation of the proteins by 15% SDS−PAGE. The tip fibrillae were collected at ~15% sucrose.

Pili preparations

In order to activate the transcription of the *pap* operon, cells carrying a plasmid with the WT operon or a mutant version of it were passaged several times (at least three) on solid CFA medium (20 g/l casamino acids, 3 g/l yeast extract, 1 mM $MgSO_4$, 0.1 mM $MnCl_2$ and 20 g/l agar) with the required antibiotics at 37°C. When preparing pili from strains containing an inducible plasmid *in trans* with a plasmid carrying a version of the operon, IPTG was added to 10 mM final concentration to 15 large plates at the last passage in order to induce the expression of either *papF*, *papK* or *papE* from the *Ptrc* or *Ptac* promotor. In each of these experiments, a control strain containing the plasmid with the operon and the pTrc99A vector *in trans* was always grown as a control in the same conditions. Pili from the strains to compare were prepared from the same amounts of cells using the following procedure: cells were scraped from plates in 2 ml (PBS) per plate, washed in PBS, resuspended in 0.5 mM Tris and 75 mM NaCl (pH 8), and heated for 30 min at 65°C. Two consecutive spins were used to remove defimbriated cells and to pellet cell debris, after which pili were precipitated from the supernatant by slowly adding NaCl to 300 mM and $MgCl_2$ to 100 mM. Pili were pelleted by centrifugation and resuspended in 20 mM Tris (pH 7.5) by rocking overnight at 4°C. These pili preparations were used for comparative quantification by ELISA. For electron microscopy the preparations were further purified by dilution to a larger volume in 75 mM NaCl and 0.5 mM Tris (pH 8), spinning to eliminate non-resuspended material and performing a second NaCl−$MgCl_2$ precipitation on the supernatant.

Hemagglutination

Piliated cells were resuspended in PBS to an absorbance of 1.0 at 540 nm, then concentrated 10-fold by centrifugation and serially diluted 2-fold in conical wells of a 96-well non-sterile Serocluster Costar plate. Human red blood cells of the P serotype were washed in PBS and resuspended to an absorbance of 1.5 at 640 nm. 25 μl aliquots of blood were distributed in the wells and the reaction was incubated for 1 h at 4°C. The HA titer was determined as the highest dilution of cells that gave rise to detectable HA.

Antisera

Purified WT tip fibrillae and purified pili were used to raise polyclonal antibodies in rabbits. The antisera were complement-inactivated by heat. Anti-pili antiserum was adsorbed repeatedly against a *papA*$^-$ strain (HB101/pPAP23, Lindberg *et al.*, 1984) to remove antibodies against minor pili subunits. Similarly, anti-tip fibrillar antiserum was adsorbed against an outer membrane preparation from HB101 to remove antibodies reacting against contaminating membrane proteins. The antisera were used at dilutions of 1:200 in Western blots and 1:100 (anti-tip fibrillar antiserum) or 1:1000 (anti-pili antiserum) respectively in Elisa tests. Western blots were performed using a standard technique (Harlow and Lane, 1988).

Comparative ELISA

Purified pili obtained from identical amounts of cells of the strains to be compared were diluted serially 2-fold in triplicate in PBS and 50 μl of each dilution were used to coat the wells of a 96-well Nunc Immunoplate overnight at 4°C. The ELISA test was performed using a standard procedure (Harlow and Lane, 1988). The plates were read using a Molecular Devices Microplate Reader at 450 nm. Curves of the absorbance as a function of the dilution of the coating antigen were drawn and the slope parts of the curves were used to compare the amount of antigen (PapA or tip proteins) between the pili of two strains obtained under exactly the same conditions. The antisera did not show any significant reactivity in ELISA against a non-piliated HB101 control strain.

Isolation of periplasmic proteins

This was performed as described in Hultgren *et al.* (1989).

Electron microscopy

Pili were prepared for electron microscopy by adsorption to mica chips that were quick-frozen, then freeze-fractured and deep-etched before rotary replication with platinum (Heuser, 1989).

Acknowledgements

We thank Jerry Pinkner for help in purifying tip fibrillae, Robin Roth and Brenda Moore for excellent technical assistance with the electron microscopy and Meta Kuehn and Hal Jones for critical reading of the manuscript. F.J.-D. is the recipient of a Long Term Postdoctoral EMBO Fellowship and K.D. of a Markey Post Doctoral Fellowship. This work was supported by grants to S.J.H. from Lucille P.Markey Charitable Trust, Washington University/ Monsanto Biomedical Research Contract, National Institutes of Health (Support Grant 1RO1AI29549), Institutional Biomedical Research (Support Grant 2-SO7-RR-5389) and the American Cancer Society (Grant IN-36).

References

Baga,M., Norgren,M. and Normark,S. (1987) *Cell*, **49**, 241−251.
Dodson,K., Jacob-Dubuisson,F., Striker,R. and Hultgren,S. (1993) *Proc. Natl. Acad. Sci. USA*, in press.
Eshdat,Y., Silverblatt,F.J. and Sharon,N. (1981) *J. Bacteriol.*, **148**, 304−314.
Gong,M. and Makowsky,J. (1992) *J. Mol. Biol.*, **228**, 735−742.
Harlow,E. and Lane,D. (1988) *Antibodies. A Laboratory Manual*. Cold Spring Harbor Laboratory Press, Cold Spring Harbor, NY.
Heuser,J. (1989) *J. Electron. Microsc. Tech.*, **13**, 244−263.
Holmgren,A., Kuehn,M., Branden,C.I. and Hultgren,S.J. (1992) *EMBO J.*, **11**, 1617−1622.
Hultgren S.J., Lindberg,F., Magnusson,G., Kihlberg,J., Tennent,J.M. and Normark,S. (1989) *Proc. Natl. Acad. Sci. USA*, **86**, 4357−4361.
Hultgren,S.J., Abraham,S.N. and Normark,S. (1991) *Annu. Rev. Microbiol.*, **45**, 383−415.
Klemm,P. and Christiansen,G. (1987) *Mol. Gen. Genet.*, **208**, 439−445.
Kuehn,M.J., Normark,S. and Hultgren,S.J. (1991) *Proc. Natl. Acad. Sci. USA*, **88**, 10586−10590.
Kuehn,M.J., Heuser,J., Normark,S. and Hultgren,S.J. (1992) *Nature*, **356**, 252−255.
Lindberg,F. (1987) Ph.D Thesis, University of Umea, Sweden.
Lindberg,F., Lund,B. and Normark,S. (1984) *EMBO J.*, **3**, 1167−1173.
Lindberg,F., Lund.,B., Johansson,L. and Normark,S. (1987) *Nature*, **328**, 84−87.
Lindberg,F., Tennent,J.M., Hultgren, S.J., Lund,B. and Normark,S. (1989) *J. Bacteriol.*, **171**, 6052−6058.
Lund,B., Lindberg,F., Marklund,B.I. and Normark,S. (1987) *Proc. Natl. Acad. Sci. USA*, **84**, 5898−5902.
Marklund,B.I., Tennent,J.M., Garcia,E., Hamers,A., Baga,M., Lindberg,F., Gaastra,W. and Normark,S. (1992) *Mol. Microbiol.*, **6**, 2225−2242.
Mc Michael,J.C. and Ou,J.T. (1979) *J. Bacteriol.*, **138**, 969−975.
Mooi,F.R., Wifjes,A. and de Graaf,F.K. (1983) *J. Bacteriol.*, **154**, 41−49.
Norgren,M., Baga,M., Tennent,J.,M. and Normark,S. (1987) *Mol. Microbiol.*, **1**, 169−178.
Oudega,B, de Graaf,M., de Boer,L., Bakker,D., Vader,C.E.M., Mooi,F.R. and de Graaf,F.K. (1989) *Mol. Microbiol.*, **3**, 645−652.

Riegman,N., van Die,I., Leunissen,J., Hoekstra,W. and Bergmans,H. (1988) *Mol. Microbiol.*, **2**, 73–80.
Riegman,N., Hoschutzky,H., van Die,I., Hoekstra,W., Jann,K. and Bergmans,H. (1990a) *Mol. Microbiol.*, **4**, 1193–1198.
Riegman,N., Acton,D., Sakkers,R., van Die,I., Hoekstra,W. and Bergmans,H. (1990b) *Mol. Microbiol.*, **4**, 101–106.
Russel,P.W. and Orndorff,P.E.(1992) *J. Bacteriol.*, **174**, 5923–5935.
Salit,I.E. and Gotshlich,E.C. (1977) *J. Exp. Med.*, **146**, 308–314.
Schifferli, D.M., Beachey,E.H. and Taylor,R.K. (1991) *J. Bacteriol.*, **173**, 1230–1240.
Schmoll,T., Hoschuetzky,H., Morschhauser,J., Lottspeich,F., Jann,K. and Hacker,J. (1989) *Mol. Microbiol.*, **3**, 1735–1744.
Simons,B.L., Willemsen,P.T.J., Bakker,D., Roosendaal,B., De Graaf,F.K. and Oudega,B. (1990) *Mol. Microbiol.*, **4**, 2041–2050.
Uhlin,B.E., Norgren,M., Baga,M. and Normark,S. (1985) *Proc. Natl. Acad. Sci. USA*, **82**, 1800–1804.
Westerlund,B., van Die,I., Kramer,C., Kuusela,P., Holthoefer,H., Tarkkanen,A.M., Virkola,R., Riegman,N., Bergmans,H., Hoekstra,W. and Korhonen,T.K. (1991) *Mol. Microbiol.*, **5**, 2965–2975.
Zhang,H., Scholl,R., Browse,J. and Somerville,C. (1988) *Nucleic Acids Res.*, **16**, 1220.

Received on July 28, 1992; revised on October 26, 1992